

Role of Hidden Neurons in A RBF Type ANN in Stream Flow Forecasting

Fernando, A. K.¹ and A. Y. Shamseldin²

¹ School of the Built Environment, Unitec New Zealand, Auckland, New Zealand,
Email: afernando@unitec.ac.nz

² Department of Civil and Environmental Engineering, The University of Auckland, Private Bag 92019,
Auckland, New Zealand Email: a.shamseldin@auckland.ac.nz

Keywords: *Radial Basis Functions, Artificial Neural Networks, Baseflow, Interflow, Surface runoff*

EXTENDED ABSTRACT

Although the use of Artificial Neural Networks (ANNs) in hydrological forecasting is widespread, the use of ANNs is occasionally treated with some scepticism due to its “Black Box” nature. Their use has posed some discomfort among some of the users of traditional models in that there is no explanation of the underlying actual hydro-meteorological processes that contribute to the modelled phenomena.

This paper intends to present the outcome of a study conducted using the data of a stream in New Zealand to illustrate that the hidden neurons in an ANN modelling tool, indeed, do have roles to play in representing the various processes involved in the hydrological phenomenon. It sheds light on the role of the hidden neurons in a Radial Basis Function (RBF) type ANN used to forecast the streamflows using the antecedent daily flow data.

It is shown that (a) the modeller can determine the level to which the hydrograph is decomposed and, therefore, the complexity of the neural network, (b) each node in the hidden layer of neurons plays a role in reconstructing the hydrograph from its components, and that (c) the contributions from the hidden layer neurons are representative of the components that make up the flow hydrograph both quantitatively and qualitatively.

It is suggested that further numerical experiments with varying catchment characteristics be carried out to make conclusive remarks regarding the shapes of the composition hydrographs and ascertain if they mimic any of the traditional flow separation techniques.

1. INTRODUCTION

Application of Multi-layer perceptron type Artificial Neural Networks (MLPANNs) in hydrological modelling began in the 1990's (Liong & Chan, 1993; Jayawardena & Fernando, 1995; Shamseldin, 1997; Maier & Dandy, 1996). The use of Radial Basis Function type ANNs (RBFANNs) followed in the late 1990's and early 2000's (Jayawardena & Fernando, 1998; Fernando & Jayawardena, 1998; Sudheer & Jain, 2003; Nor, Harun, & Kassim, 2007). Comparisons of the MLPANN and RBFANN in terms of prediction accuracy has also been established (Jayawardena, Fernando, & Zhou, 1996; Gupta, Sorooshian, Hsu, & Moradkhani, 2004; Garbrecht, 2006).

Despite the success of the ANN based models, a major challenge to the ANN enthusiasts is the reluctance in the wider hydrological community to accept this approach as an alternative to traditional modelling. The hesitation arises mainly due to the lack of understanding of the internal functioning of the so-called *hidden* nodes in the ANNs. The *Black-box* nature of the model and mere focus on large amounts of data while completely disregarding the hydrological processes underlying the phenomenon modelled contribute to the uncertainties surrounding this approach. De Vos & Rientjes (2005) pointed out the need for advanced research on ANNs to realise their full potential in hydrological modelling.

In the recent past several researchers have attempted to explain the internal functioning of the ANNs and extract relevant knowledge from the final trained network (Dibike, Solomatine, & Abbott, 1999; Jain, Sudheer, & Srinivasulu, 2004; Shamseldin, Abrahart, & See, 2005; Wilby, Abrahart, & Dawson, 2003). These have focussed on the MLPANN and to extant knowledge, there are no reported attempts to understand the internal functioning of the RBFANNs.

The work presented in this paper is an attempt at a logical interpretation of the internal functioning of a RBFANN. Section 2 of this paper gives a brief description of the RBFANN architecture used in the study, Section 3 describes the application and the results, and finally, in Section 4, a brief discussion and the conclusions are presented.

2. RBF NETWORK

Radial Basis Function type ANN owes its name to the transfer function applied at its hidden neurons.

An RBFANN used in this study has one input layer with three nodes (inputs), a single hidden layer (with M nodes) and one output. For the p^{th} input pattern $\mathbf{X}^p = [x_{p1} \ x_{p2} \ x_{p3}]$ if the RBF centres are $U_1 = [u_{11}, u_{12}, u_{13}]$, $U_2 = [u_{21}, u_{22}, u_{23}] \dots U_j = [u_{j1}, u_{j2}, u_{j3}]$, then, the response of the j^{th} hidden neuron h_{pj} is given by

$$h_{pj} = \exp \left\{ - \left(\frac{(x_{p1} - u_{j1})^2}{2\sigma_j^2} + \frac{(x_{p2} - u_{j2})^2}{2\sigma_j^2} + \frac{(x_{p3} - u_{j3})^2}{2\sigma_j^2} \right) \right\} \quad (1)$$

The contribution from each hidden node to the output, out_{pj} , is the product of hidden response and the weight of the output layer synaptic connection w_j , i.e.,

$$out_{pj} = h_{pj} \times w_j \quad (2)$$

and the RBF network output z_p for the p^{th} pattern is given by

$$z_p = \sum_{j=1}^M out_{pj} \quad (3)$$

The parameters of the RBF (i.e. the centre U_j and spread σ_j) together with the output layer weights w_j constitute the network parameters. Accordingly, the calibration of the RBF network model entails determining the most appropriate values for these parameters.

To evaluate the role of each hidden node, the proportional contribution from each node, the ratio $PC_j = out_{pj}/z_p$ was computed.

3. APPLICATION

The application in this study is to perform the hourly forecast of flow in the Kapakapanui Stream approximately 300m upstream of its confluence with the Waikanae River in Porirua, Wellington, New Zealand. Hourly flow has been estimated from water levels measured at 15min intervals at a level gauge installed in the stream. The measurements were carried out from July 1998 to September 1999 using standard gauging methods set out in the Water Resources Survey-Hydrologists Field Manual DSIR (1991). Table 1 summarises the characteristics of the flow data used from the collection.

Table 1. Measured flow characteristics

	Start	End	Maximum flow (L/s)	Minimum flow (L/s)
Event 1	5/10/1998 16:15	8/11/1998 13:15	13209	126
Event 2	21/07/1998 15:35	23/08/1998 11:35	5095	132
Event 3	30/08/1998 14:05	3/10/1998 8:05	4979	110
Event 4	11/05/1999 20:45	11/06/1999 2:45	10030	58
Event 5	16/08/1999 13:15	5/09/1999 16:15	7954	100

The dry weather flow in the Kapakapanui stream is fairly low (<500 L/s) and its catchment displays a fast response to rainfall with heavy fluctuations in its flow hydrograph.

The input vector to the RBFANN model is made up of the antecedent flow rates $Q(t)$, $Q(t-1)$, and $Q(t-2)$, the output is the one-dimensional forecast flow rate $Q(t+1)$, where t is in hours.

3.1. Training

Event 1 (in Table 1) was chosen as the training set and the remaining four as testing sets. Determination of the optimum RBFs for the hidden layer nodes, and output layer weights was completed using a conjugate gradient method with its objective to minimise the total square error of the forecast flow for the event, i.e., the sum of $(\text{Actual flow} - \text{Forecast flow})^2$.

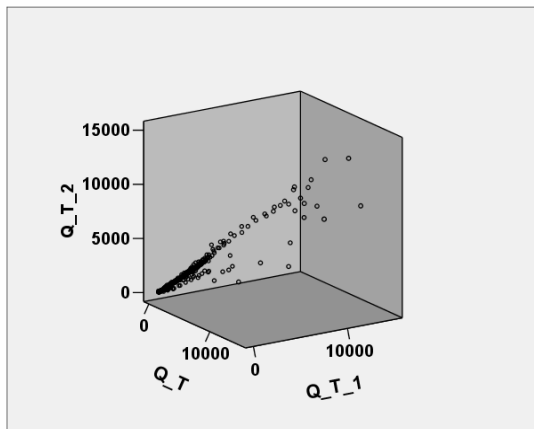


Figure 1. The input vectors in the 3-D input space [Notation: $Q_T = Q(t)$, $Q_{T_1} = Q(t-1)$, $Q_{T_2} = Q(t-2)$]

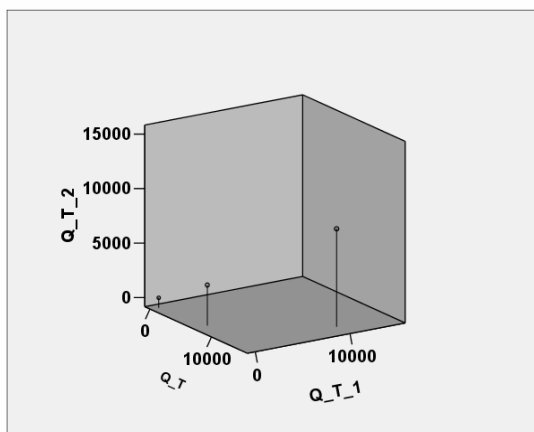


Figure 2. RBF Centres in the 3-D input space [Notation: $Q_T = Q(t)$, $Q_{T_1} = Q(t-1)$, $Q_{T_2} = Q(t-2)$]

Figures 1 and 2 demonstrate the distribution of the input data and the three selected RBF centres in

the input space. The case shown in Figure 2 is when the RBFANN architecture has three hidden nodes. As can be seen from the figure, the three centres are spatially distributed and span the entire input space. The numerical values of these RBF parameters are tabulated below (Table 2).

Table 2. RBF Parameters

RBF Centre (i)	U_{j1}	U_{j2}	U_{j3}	σ_j
1	57.5	57.5	57.5	57.5
2	2857.6	770.2	6858.8	3445.1
3	8116.3	10190.4	13367.1	8279

Figure 3 which plots the actual and forecast flows for the training set illustrates that the forecast flow closely follows the actual values. The correlation coefficient R^2 for this is high at 0.9567. The R^2 for a naïve model prediction is 0.9.

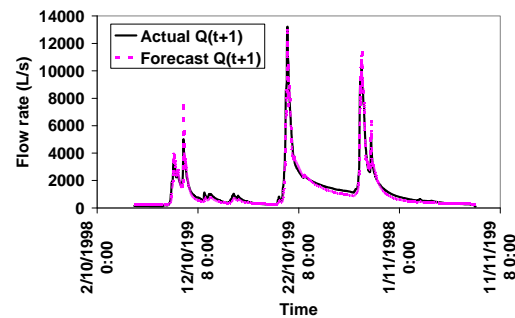


Figure 3. Comparison of actual observed and forecast flows for the training event.

3.2. Testing

Upon “calibrating” the model, the RBFANN was used to make forecasts for the remaining 4 events. When all events are concatenated the proportional contributions (PC) from each node are plotted in the Figure 4 below.

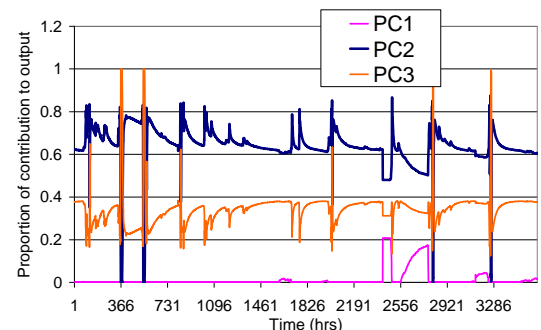


Figure 4. Proportional contributions (PC) from hidden nodes towards forecast flow for all 5 events

A dominance effect becomes apparent as PC₂ (the proportional contribution from Hidden node 2) amounts to more than 60% most of the time while node 3 supplements by up to 40%. The node 1, in contrast makes little or no contribution most of the time but contributes up to 20% which is found to be when forecasting very low flows.

The Figure 5 shows the actual hidden layer responses for Event 4 (where the lowest flows occur) on the primary axis and the observed and forecast flows on the secondary axis. This shows that the node 1 is predominantly active in the very low domain, the node 2 in medium flow range and node 3 when the flow rates are high.

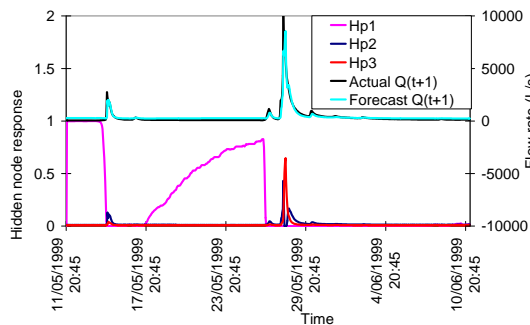


Figure 5. Hidden layer node responses and flow rates for Event 4.

Figure 6 on the other hand, shows the final proportional contributions from each hidden node towards the forecast flow (on the primary axis) and the actual and forecast flows (on the secondary axis) for Event 4 only. This clearly demonstrates that node 2 contributes to the forecast dominantly throughout the event, switching the dominance to node 3 only when the high flows are forecast.

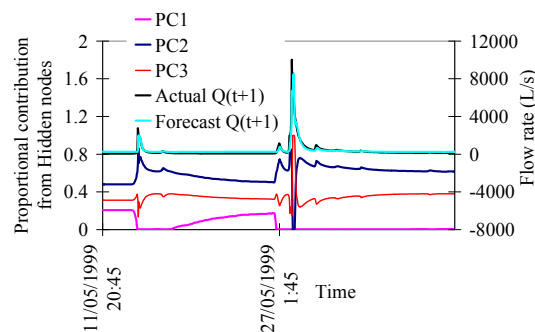


Figure 6. Proportional contributions (PC) from hidden nodes towards forecast flow for Event 4.

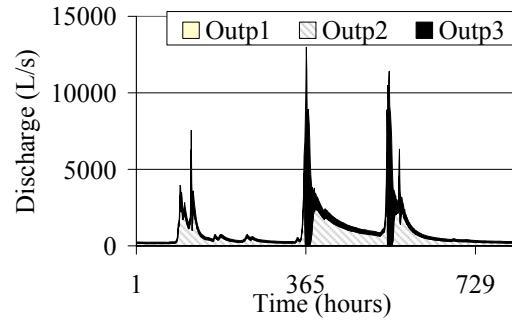


Figure 7. Flow components as modelled by hidden nodes in forecasting flow in the training event

Figures 7 and 8 show the actual contributions towards the total flow for the training event and Event 4 respectively. These show how the individual contributions stack up to synthesise the flow hydrograph. According to Figure 7, the flow forecasting model representation breaks-down the flow domain into two regions – low and high, with the contribution from the node 1, Out_{p1}, almost non-existent. The hidden nodes activate and make contributions towards the forecast at certain thresholds of flow. In the case of the training event, this threshold is ~2000 L/s. For the Event 4, which has the lowest flows (see Table 1) Out_{p1} also becomes significant in the low flow regions as demonstrated in Figure 8 where the y axis is exaggerated to show the lowest flow region. The flow domain in this case has been spilt into low, medium and high.

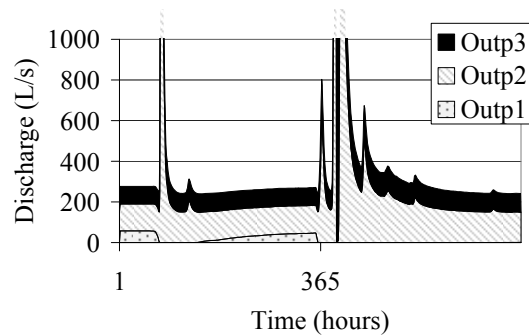


Figure 8. The flow components as modelled by hidden nodes in Event 4 in its low flow region.

Table 3 summarises the statistics of the forecasts. While the peak error is within an acceptable range, the root mean square (RMS) error expressed as a percentage of the mean flow rate becomes as high as 78.2% for Event 4 mainly due to the poor forecasting accuracy at the low flow range; low flow values are dominant in all the testing events.

Table 3. Statistics for the performance of the RBFANN for the events (Event 1: training set).

	Peak error %	Mean flow rate (L/s)	RMS Error expressed as a % of the actual mean
Event 1	1.7	1279	28.4
Event 2	-11.2	469	39.7
Event 3	-14.5	316	47.8
Event 4	14.6	343	78.2
Event 5	-6.3	381	69.4

3.3. Training and testing with 2 hidden nodes

The appropriate number of hidden nodes is not known *a priori*. Determination of this number is not the focus of this study. However, how the internal functioning of the hidden nodes would differ if fewer nodes (in this case only two) were used was tested next. The same events, as before, were used for training and testing.

Table 4 summarises the error statistics for this experiment which illustrates that the accuracy of the model predictions are of the same order and has not suffered as a result of the reduced number of hidden nodes.

Table 4. Statistics for the performance of the RBFANN with two hidden nodes (Event 1 : Training set).

	Peak error %	RMS Error expressed as a % of the actual mean
Event 1	2.6	27.5
Event 2	-13.8	37.0
Event 3	-15.0	48.7
Event 4	12.7	75.8
Event 5	-9.0	70.4

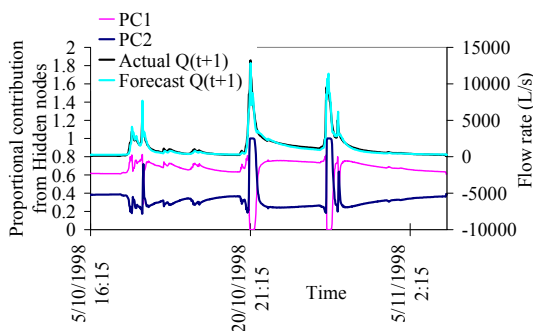


Figure 9. The proportional contributions from two hidden nodes for the training set.

Figure 9 illustrates that the proportional contributions from the two hidden nodes is such that the node 1 predominantly contributes (about 60%) in the low flow region and the node 2 dominates in the peak flow regions with the

switch-over of the dominance occurring at ~1000L/s threshold. It is also noted that, in the rising and falling limbs of the hydrograph below the threshold, contribution from node 1 (PC1) increases while that of node 2 decreases.

It can be observed from Figure 10 for Event 4 that the flow hydrograph is now made up of a low flow component (what seems like the base flow) contributed entirely by the hidden node 1 and a high flow component.

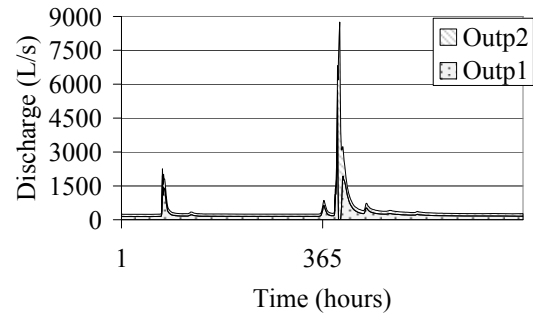


Figure 10. The flow components of Event 4 as modelled by RBFANN with two hidden nodes.

4. DISCUSSION AND CONCLUSIONS

If three hidden nodes are used for representing the flow regime, it appears that the third fails to make a significant contribution except in the very low flow regime. Knowing that the RBFs are distributed in the input space and that their contributions are significant in specific flow thresholds gives an opportunity to the modeller to use an appropriate number of hidden nodes by using the prior knowledge regarding the stream flow characteristics. In Kapakapanui stream/catchment where the dry weather flow is low (<500 L/s) and fast response to rainfall is displayed, a 2-noded hidden layer appear to suffice to mimic the base flow and the high flow components and fluctuations in the flow hydrograph in response to rainfall.

The activation of the hidden nodes is not random; it follows a pattern that is dictated by the underlying data and in turn, the underlying hydrological process. The observations in this experiment clearly demonstrate that the hidden node contributions make up the flow components which collectively represent the total flow hydrograph. However, further numerical experiments with various types of catchments are necessary to make more conclusive remarks regarding the shape of the composition hydrographs and how they represent the traditional

equations for the flow components of base flow, interflow and surface flow.

5. REFERENCES

- De Vos, N. J., & Rientjes, T. H. M. (2005). Constraints of artificial neural networks for rainfall-runoff modelling: trade-offs in hydrological state representation and model evaluation. *Hydrology and Earth System Sciences*, 9, 111-126.
- DSIR(Christchurch). (1991). *Water Resources Survey - Hydrologists Field Manual, Quality Manual*.
- Fernando, D. A. K., & Jayawardena, A. W. (1998). Runoff forecasting using RBF networks with OLS algorithm. *Journal of Hydrologic Engineering*, 3(3), 203-209.
- Garbrecht, J. D. (2006). Comparison of three alternative ANN designs for monthly rainfall-runoff simulation. *Journal of Hydrologic Engineering*, 11(5), 502-505.
- Gupta, H. V., Sorooshian, S., Hsu, K. L., & Moradkhani, H. (2004). Improved streamflow forecasting using self-organizing radial basis function artificial neural networks. *Journal of Hydrology (Amsterdam)*, 295(1/4), 246-262.
- Jain, A., Sudheer, A. P., & Srinivasulu, S. (2004). Identification of physical processes inherent in artificial neural network rainfall runoff models. *Hydrological Processes*, 18, 571-581.
- Jayawardena, A. W., & Fernando, D. A. K. (1995). Artificial Neural Networks in hydrometeorological modelling. *Proceedings of the Fourth International conference on the application of Artificial Intelligence to Civil and Structural Engineering - Developments in Neural Networks and evolutionary computing in Civil and Structural Engineering*, Cambridge, UK.
- Jayawardena, A. W., & Fernando, D. A. K. (1998). Use of Radial Basis Function Type Artificial Neural Networks for Runoff Simulation. *Computer-Aided Civil and Infrastructure Engineering*, 13(2), 91-99.
- Jayawardena, A. W., Fernando, D. A. K., & Zhou, M. C. (Eds.). (1996). *Comparison of multilayer perceptron and radial basis function network as tools for flood forecasting*. Anaheim, California: IAHS Red Book series.
- Liong, S. Y. and Chan, W. T. (1993) Runoff volume estimates with neural networks. In Topping, B. H. V. and Khan, A. I., editors, *Proceedings of the 3rd International Conference on the Application of AI to Civil and Structural Engineering*, Edinburgh: Civil Computer Press, 67-70
- Maier, H. R., & Dandy, G. C. (1996). Use of Artificial Neural Networks for the Prediction of Water Quality Parameters. *Water Resources Research*, 32(4), 1013-1022.
- Nor, I. A. N., Harun, S., & Kassim, A. H. M. (2007). Radial Basis Function Modeling of Hourly Streamflow Hydrograph. *Journal of Hydrologic Engineering*, 12(1), 113-123
- Shamseldin, A. Y. (1997). Application of neural network technique to rainfall-runoff modelling. *Journal of Hydrology*, 199: 272-294.
- Shamseldin, A.Y., Abrahart, R.J. and See, L.M. (2005) Neural network river discharge forecasters: An empirical investigation of hidden unit processing functions based on two different catchments. *Proceedings of the International Joint Conference on Neural Networks*, Montreal, 31 Jul - 4 Aug 2005.
- Sudheer, K. P., & Jain, S. K. (2003). Radial Basis Function Neural Network for Modeling Rating Curves. *Journal of Hydrologic Engineering*, 8(3), 161-164.